

Experimental study of the energy and exergy performance for a pressurized volumetric solar receiver

Zhu, Jianqin; Wang, Kai; Li, Guoqing; Wu, Hongwei; Jiang, Zhaowu; Lin, Feng; Li, Yongliang

DOI:

[10.1016/j.applthermaleng.2016.05.075](https://doi.org/10.1016/j.applthermaleng.2016.05.075)

License:

Creative Commons: Attribution-NonCommercial-NoDerivs (CC BY-NC-ND)

Document Version

Peer reviewed version

Citation for published version (Harvard):

Zhu, J, Wang, K, Li, G, Wu, H, Jiang, Z, Lin, F & Li, Y 2016, 'Experimental study of the energy and exergy performance for a pressurized volumetric solar receiver', *Applied Thermal Engineering*, vol. 104, pp. 212-221. <https://doi.org/10.1016/j.applthermaleng.2016.05.075>

[Link to publication on Research at Birmingham portal](#)

Publisher Rights Statement:

Checked 12/7/2016

General rights

Unless a licence is specified above, all rights (including copyright and moral rights) in this document are retained by the authors and/or the copyright holders. The express permission of the copyright holder must be obtained for any use of this material other than for purposes permitted by law.

- Users may freely distribute the URL that is used to identify this publication.
- Users may download and/or print one copy of the publication from the University of Birmingham research portal for the purpose of private study or non-commercial research.
- User may use extracts from the document in line with the concept of 'fair dealing' under the Copyright, Designs and Patents Act 1988 (?)
- Users may not further distribute the material nor use it for the purposes of commercial gain.

Where a licence is displayed above, please note the terms and conditions of the licence govern your use of this document.

When citing, please reference the published version.

Take down policy

While the University of Birmingham exercises care and attention in making items available there are rare occasions when an item has been uploaded in error or has been deemed to be commercially or otherwise sensitive.

If you believe that this is the case for this document, please contact UBIRA@lists.bham.ac.uk providing details and we will remove access to the work immediately and investigate.

Accepted Manuscript

Experimental Study of the Energy and Exergy performance for a Pressurized Volumetric Solar Receiver

Jianqin Zhu, Kai Wang, Guoqing Li, Hongwei Wu, Zhaowu Jiang, Feng Lin, Yongliang Li

PII: S1359-4311(16)30732-3

DOI: <http://dx.doi.org/10.1016/j.applthermaleng.2016.05.075>

Reference: ATE 8290

To appear in: *Applied Thermal Engineering*

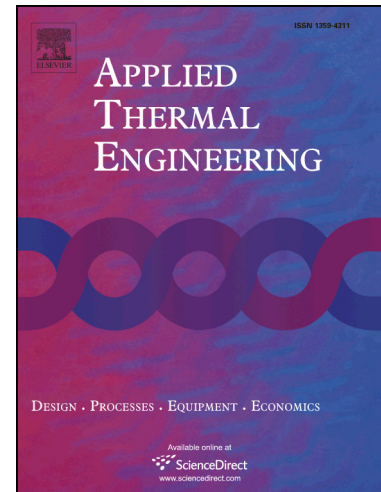
Received Date: 23 March 2016

Revised Date: 13 May 2016

Accepted Date: 13 May 2016

Please cite this article as: J. Zhu, K. Wang, G. Li, H. Wu, Z. Jiang, F. Lin, Y. Li, Experimental Study of the Energy and Exergy performance for a Pressurized Volumetric Solar Receiver, *Applied Thermal Engineering* (2016), doi: <http://dx.doi.org/10.1016/j.applthermaleng.2016.05.075>

This is a PDF file of an unedited manuscript that has been accepted for publication. As a service to our customers we are providing this early version of the manuscript. The manuscript will undergo copyediting, typesetting, and review of the resulting proof before it is published in its final form. Please note that during the production process errors may be discovered which could affect the content, and all legal disclaimers that apply to the journal pertain.



Experimental Study of the Energy and Exergy performance for a Pressurized Volumetric Solar Receiver

Jianqin Zhu^a, Kai Wang^{b,*}, Guoqing Li^b, Hongwei Wu^{c,**},
Zhaowu Jiang^b, Feng Lin^b, Yongliang Li^d

^a National Key Lab. of Science and Technology on Aero-Engines,
School of Energy and Power Engineering, Beihang University, Beijing 100191, China

^b Institute of Engineering Thermophysics, Chinese Academy of Sciences,
Beijing, 100190, China.

^c Department of Mechanical and Construction Engineering, Faculty of Engineering and Environment,
Northumbria University, Newcastle upon Tyne, NE1 8ST, United Kingdom

^d School of Chemical Engineering, University of Birmingham,
Edgbaston, Birmingham B15 2TT United Kingdom

*Corresponding author. Email: wang_kai@iet.cn Tel. +86(10)82543147 Fax. +86(10)82613328

**Corresponding author. Email: hongwei.wu@northumbria.ac.uk Tel. +44(0)1913495365

Abstract

This article presents an experimental investigation of the heat transfer characteristics as well as energy and exergy performance for a pressurised volumetric solar receiver under variable mass flow rate conditions. During a two-hour period of continuous operation in the morning, the solar irradiance is relatively stable and maintained at approximately 600 W/m^2 , which is beneficial for analyzing the energy and exergy performance of the solar receiver. Experimental results show that the mass flow rate fluctuation has insignificant effect on the solar receiver outlet temperature, whereas the mass flow rate plays an important role in the solar receiver power, energy efficiency and exergy efficiency. The efficiency of the solar receiver is normally above 55% with the highest efficiency of 87%, and under steady state operating conditions the efficiency is maintained at approximately 60%. A very low value of the

heat loss factor (0.014 kW/K) could be achieved during the current steady state operating conditions. The highest exergy efficiency is approximately 36%. In addition, as the temperature difference increases, the impact of the exergy factor increases. The highest exergy factor is 0.41 during the entire test.

Keywords: solar receiver; exergy; energy efficiency; heat transfer; radiation.

Nomenclature

A_{ap}	effective aperture area of dish [m ²]	δEx_R	uncertainty of the receiver exergy rate [-]
A_p	project area [m ²]	G	direct solar radiation [W/m ²]
c_{av}	average specific heat capacity [J/kg·K]	\dot{m}	mass flow rate [kg/s]
C_p	Solid specific heat capacity [J/kg·K]	n_d	parabolic dish combined optical efficiency [-]
D_f	focus point diameter [m]	r_c	concentration ratio
E_D	concentrated solar radiation power [kW]	T_{in}	inlet temperature of the air [K]
E_L	heat loss [kW]	T_{out}	outlet temperature of the air [K]
E_R	receiver power [kW]	T_{ave}	average temperature of the air [K]
E_S	solar radiation power on the dish [kW]	T_s	surface temperature of the sun [K]
Ex_D	rate of dish exergy concentrated [kW]	T_{amb}	ambient temperature [K]
Ex_f	exergy factor [-]	U_L	heat loss coefficient [kW/m ² K]
Ex_R	receiver exergy [kW]	$\eta_{th.R}$	energy efficiency of the receiver [-]
Ex_S	rate of solar exergy delivery [kW]	$\eta_{ex.R}$	exergy efficiency of the receiver [-]
δE_R	uncertainty of the receiver power [-]		

1. Introduction

With rapidly increasing energy prices and globalization, process industries seek opportunities to reduce production costs and improve energy efficiency. Among the energy-efficient technologies, Concentrated Solar Power (CSP) system is considered as one of the most attractive ways to solve the energy crisis in the future [1,2]. Many developed countries like the United State and the European Commission have been devoted to the solarized Brayton micro-turbines system over the past decades [3-5].

Compared to the traditional gas turbine, solarized Brayton turbines use a solar receiver to replace the combustion chamber in the traditional gas turbine [6]. The solar concentration part which is used to provide high temperature air is very crucial for the entire solar power system. The system efficiency and the cost of the power generation are highly depended on the solar concentration conversion efficiency from solar radiation to the thermal fluid. Thus, the solar concentration part has to be well designed in order to achieve high efficiency and low pressure loss. Many studies have been devoted to the design and performance of the receiver. Neber and Lee [7] designed a high temperature cavity receiver using silicon carbide. Then a scaled test section was placed at the focal point of a parabolic dish collector and reached a maximum temperature of 1248 K. Lim et al. [8] designed a tubular solar receiver with a porous medium and found the optimal design point of the proposed solar receiver concept to heat up compressed air. The results of this study offer a valuable design guideline for future manufacturing processes. Wu et al. [9] developed a novel particle

receiver concept for concentrating solar power (CSP) plants. Special attention was paid to the effect of rotation on convective flow in a cylindrical cavity with heated side walls for solar applications. Buck et al. [10] introduced a receiver module consisting of a secondary concentrator and a volumetric receiver unit which was closed with a domed quartz window to transmit the concentrated solar radiation. Hischer et al. [11, 12] proposed a novel design of a high-temperature pressurized solar air receiver for power generation via combined Brayton-Rankine cycles. It consists of an annular reticulate porous ceramic bounded by two concentric cylinders. The heat transfer mechanism was analyzed by the finite volume technique and by using the Rosseland diffusion, P1, and Monte-Carlo radiation methods. It was found that, for a solar concentration ratio of 3000 suns, the outlet air temperature can reach 1000 °C at 10 bars, yielding a thermal efficiency of 78%.

It is recognized that the flow and heat transfer processes in the solar receiver are very complicated. Over the past years, many studies have been devoted to the optimization of the design using theoretical and numerical methods. Nan Tu et al. [13] studied a saturated water/steam solar cavity receiver with different depths by adopting a combined computational model. Various trends of thermal efficiency and heat loss with depths were obtained. A suitable cavity depth was finally found for the receiver. Wang and Siddiqui [14] developed a three-dimensional model of a parabolic dish-receiver system with argon gas as the working fluid to simulate the thermal performance of a dish-type concentrated solar energy system. Wu et al. [15] presented

and discussed temperature and velocity contours as well as the effects of aperture position and size on the natural convection heat loss. Their study revealed that the impact of aperture position on the natural convection heat loss is closely related to tilt angle, while the aperture size has a similar effect for different tilt angles. Hachicha et al. [16, 17] proposed a numerical aerodynamic and heat transfer model based on Large Eddy Simulation (LES) modelling of parabolic trough solar collectors (PTC), and verified the numerical model on a circular cylinder in the cross flow. The circumferential distribution of the solar flux around the receiver was also studied. Von Storch et al. [18] proposed a process for indirectly heated solar reforming of natural gas with air as heat transfer fluid. Different solar receivers were modeled and implemented into the reforming process.

On the other hand, many numerical research works are also conducted to simulate the detail heat transfer process. Flesch et al. [19] numerically analyzed the impact of head-on and side-on wind on large cavity receivers with inclination angles ranging from 0° (horizontal cavity) to 90° (vertical cavity) and compared with the data published in the open literature. Yu et al. [20] performed a numerical investigation on the heat transfer characteristics of the porous material used in the receiver of a CSP with different structure parameters. The effects of different boundary conditions were revealed. Tu et al. [21] proposed a modified combined method to simulate the thermal performance of a saturated water/steam solar cavity receiver. Capeillere et al. [22] numerically studied the thermomechanical behavior of a plate solar receiver with

asymmetric heating. The numerical results showed that the choice of the shape and levels of the solar irradiance map is crucial. The distribution of the most relevant incident solar flux and the geometry compromise were determined. Wang et al. [23] conducted a numerical study focusing on the thermal performance of a porous medium receiver with quartz window. Their results indicated that the pressure distribution and temperature distribution for the condition of fluid inlet located at the side wall was different from that for the condition of fluid inlet located at the front surface. Roldan et al. [24] carried out a combined numerical and experimental investigation of the temperature profile in the wall of absorber tubes of parabolic-trough solar collectors using water and steam as the heat-transfer fluids. A good agreement between the measured and computed thermal gradient was achieved.

Exergy analysis has been applied in various power studies. In the authors' earlier studies [25, 26], a coiled tube solar receiver had been designed and tested in the real solar radiation condition. But due to the limitation of the tube material, the coiled tube solar receiver could not achieve very high temperature. Thus, a pressurized volumetric solar receiver using metal foam as thermal absorbing core is designed in this work. It appears from the previous investigation that the key point for the solarized Brayton micro-turbines is to develop solar receivers which have exemplary performance on the pressure loss and heat transfer. To the best of the authors' knowledge, there is a lack of available experimental data under real concentrated solar and variable mass flow conditions especially for the cases of extremely high heat flux

and high temperature. To this end, the present research is aimed to experimentally analyze both the efficiency and heat loss of a pressurized volumetric solar receiver under real solar radiation and variable mass flow conditions in more detail.

2. Experimental apparatus and method

2.1. Experimental apparatus

The experimental study was conducted at a location with the geographical position of 30°36' latitude and 120°22' longitude, Hangzhou, China. The whole system, shown schematically in Fig. 1, mainly consists of three components: dish, compressor and receiver. The dish used for the experimental tests of the developed solar heat receiver is shown in Fig. 2. All 40 trapezoidal, pre-bent mirrors are resin molded and laminated. The reflective surface is applied as an adhesive foil. At the bottom of the dish a cut out is made for the tower. The main dish parameters utilized in the current study are illustrated in Table 1, which is provided by the dish reflector manufacturer. To make sure that the light reflected by the mirror focuses on the aperture of the receiver, each mirror was adjusted carefully.

The dish is controlled by a solar tracker which is embedded in the inner program to make the dish face the Sun automatically. The inner program could accurately calculate the attitude angle in terms of the dish location of the earth and the local time. As illustrated in Fig. 1, the attitude angle is formed between the boom line and horizon line. A stepping motor can be well controlled to change the dish attitude angle slowly. When the dish is in operation during the morning, the attitude angle is lower

than 40° for the sun just rising over the horizontal line. Whereas the dish is operated in the noon, the attitude angle is approximately 80° . It should be recognized that the initial setting for the location and accurate time is very crucial during the test. An uninterruptible power supply (UPS) system is also adopted to assist the dish off the solar direction in some emergency to further protect the receiver. During the experiments, a 20 kW piston compressor driven by electricity is used to compress the air. The pressurized air is compressed at environmental temperature from environmental pressure. After the filter, the air is pressurized into the air tank with pressure of 0.8 Mpa (absolute pressure) to guarantee enough air flow during the experiment process. After that, the pressurized air is supplied into the receiver. Two valves are installed at the receiver inlet and outlet to ensure the receiver works under the designed pressure about 0.4 Mpa. Because the light incident surface of the receiver is made of quartz glass, too high pressure could damage the receiver. Hence, by adjusting this valve, the pressure of the whole system as well as the portion of the receiver can be well controlled. The output mass flow rate is variable. Thermocouple and pressure sensor are placed at the inlet and outlet of the pipe respectively to obtain the receiver efficiency and heat loss. The receiver itself is mounted onto the cantilever arm. In the current study, the heat flux of the focus power could achieve 1000 kW/m^2 for the dish concentrator with the concentrate ratio of 1750. It can be expected that, except for the receiver and protecting panel, other components of the system would be burned in a short time. To protect other parts of the receiver from misaligned radiation,

an additional protecting panel is mounted circumferentially to the receiver. As shown in Fig. 3, the protecting panel is made of Calcium silicate board 10 mm in thickness. The diameter of the aperture in the protecting panel is 250 mm. Four K-type thermocouples with an accuracy of 0.5 °C are fixed on the back to monitor the temperature of the protecting panel. When the temperature is over 850 °C, it means that the concentrated solar spot is not located into the aperture. As a result, the inner program has to be reset to adjust the attitude angle in order to prevent fatal damage.

2.2. Solar receiver set-up

For the current experimental evaluation, as shown in Fig. 4, the solar receiver is designed as a type of pressurized volumetric solar receiver. Fig. 4(a) shows the 3D view of the model and Fig. 4(b) presents the cross section view of the receiver. The advantage of the pressurized volumetric solar receiver is high outlet air temperature and high thermal efficiency. It should be stressed here that the key point for the design of the pressurized volumetric solar receiver is the cooling of the light incident glass and the equally distributed mass flow in the heat absorbing core. The light incident glass is made of quartz glass which can endure a temperature up to 1200 C°. But the concentrated solar focuses on the quartz glass directly, the glass cooling using the inlet air could extend the life span of the receiver and make the receiver working process more secure. For this reason, a large inlet tube is used with the diameter of 50 mm. The pressurized air is injected into the inlet tube, and then, it is divided into three small tubes with a diameter of 20 mm. The three small tubes that are circumferentially

uniformly distributed are welded at the end of the pressure cavity which forms the main part of the solar receiver. The air flows along the edge of the cavity and is injected onto the quartz glass providing cooling of the light incident glass. The diameter and the height of the main part of the receiver are 400 mm and 360 mm, respectively. The concentrated solar radiation (CSR) passes through the quartz glass and heats the absorbing core. As shown in Fig. 5, the material of the absorbing core is Nickel foam which could endure a temperature up to 1453 °C. To increase the absorbing ability, 65mm Nickel foam with the PPI (Pores per Inch) value of 75 is selected. PPI which is a common parameter is usually used in industry to indicate the pore diameter of a metal foam. The 75 PPI value means that the pore diameter is about 0.34 mm. One can imagine that the small pore diameter would enhance the heat transfer coefficient and heat transfer area. At last, to minimize the heat loss, the receiver is surrounded by Aluminum silicate whose heat conductivity coefficient is 0.06 W/(m · K).

2.3. Energy and exergy analysis

Experimental energy and exergy parameters to characterize the thermal performance of the receiver are presented in this section.

2.3.1. Energy analysis [27, 28]

The energy that the whole system receives comes from the solar radiation. The solar radiation power on the parabolic dish reflector can be expressed as:

$$E_S = A_{ap} G \quad (1)$$

where E_S is the solar radiation power on the dish, A_{ap} is the effective aperture area of the parabolic dish, and G is the direct solar irradiation from the Sun to the dish. G is measured with a normal incidence pyrheliometer (NIP) Hukseflux DR01 attached to the solar tracker.

The solar radiation is concentrated and delivered to the receiver by the parabolic dish. The concentrated solar radiation power (E_D) can be expressed as:

$$E_D = n_d E_S = n_d A_{ap} G \quad (2)$$

where E_D is the concentrated solar radiation power from parabolic dish to the receiver, n_d is the parabolic dish combined optical efficiency described in Table 1.

The concentrated solar radiation on the receiver is absorbed by the heat-transfer fluid flowing in the pressurized cavity of the receiver. The energy rate that air absorbs or receives power is given by:

$$E_R = \dot{m} c_{av} (T_{out} - T_{in}) \quad (3)$$

where \dot{m} is the mass flow rate of the air, c_{av} is the average specific heat capacity of the air which is a function of the average air inlet temperature (T_{in}) and air outlet temperature (T_{out}). The average temperature of the receiver (T_{ave}) can be defined by:

$$T_{ave} = (T_{in} + T_{out})/2 \quad (4)$$

Thus, the relation between the average specific heat capacity of the air and the average temperature can be obtained as:

$$c_{av} = 0.9227 + 0.0002185T_{ave} \quad (5)$$

Eq. (5) is fitted according to the air property table from 100°C to 500°C. The unit of c_{av} is $\text{kJ}/(\text{kg} \cdot \text{K})$ and the unit of T_{ave} is K.

Based on energy conservation, the receiver power is the difference between the concentrated solar radiation power and the overall heat losses are relative low. The receiver power can also be described as

$$E_R = E_D - E_L \quad (6)$$

where E_L is the rate of the heat loss from the receiver to the surroundings, which contains the convective heat losses, conductive heat losses and radiative heat losses. E_L can be expressed as

$$E_L = U_L A_R (T_{ave} - T_{amb}) \quad (7)$$

where U_L is the total heat loss coefficient determined, A_R is the effective receiver area, and T_{amb} is the ambient temperature. The product $U_L A_R$ is referred as the heat loss factor given by

$$U'_L = U_L A_R \quad (8)$$

Therefore, combination of Eqs (2), (3), (6) and (7) can yield

$$\dot{m} c_{av} (T_{out} - T_{in}) = n_d A_{ap} G - U'_L (T_{ave} - T_{amb}) \quad (9)$$

The thermal energy efficiency of the receiver is defined as the ratio of the receiver power to the concentrated solar radiation power from the parabolic dish to the receiver which is expressed as:

$$\eta_{th.R} = \frac{E_R}{E_D} = \frac{\dot{m} c_{av} (T_{out} - T_{in})}{n_d A_{ap} G} \quad (10)$$

By dividing $A_{ap} G$ on both side of Eq. (9) and combine with Eq. (10) leads to

$$\eta_{\text{th.R}} n_d = n_d - \frac{U_L'(T_{\text{ave}} - T_{\text{amb}})}{A_{\text{ap}} G} \quad (11)$$

2.3.2 Exergy analysis [27, 28, 29]

The exergy rate of the receiver or the quality of the energy delivered to the circulating fluid with reference to the surroundings can be expressed as

$$EX_R = E_R - \dot{m} c_{\text{av}} T_{\text{amb}} \ln\left(\frac{T_{\text{out}}}{T_{\text{in}}}\right) \quad (12)$$

Substituting Eq. (3) into Eq. (12) yields

$$EX_R = \dot{m} c_{\text{av}} \left[(T_{\text{out}} - T_{\text{in}}) - T_{\text{amb}} \ln\left(\frac{T_{\text{out}}}{T_{\text{in}}}\right) \right] \quad (13)$$

The rate of the solar exergy delivery by the Sun to the dish and then to the concentrator is given by the Petela expression [30] and is expressed as

$$EX_S = GA_{\text{ap}} \left[1 + \frac{1}{3} \left(\frac{T_{\text{amb}}}{T_s} \right)^4 - \frac{4T_{\text{amb}}}{3T_s} \right] \quad (14)$$

where T_s is the surface temperature of the Sun which is approximately 5762 K.

So the concentrated solar radiation exergy (EX_D) can be expressed as:

$$EX_D = n_d GA_{\text{ap}} \left[1 + \frac{1}{3} \left(\frac{T_{\text{amb}}}{T_s} \right)^4 - \frac{4T_{\text{amb}}}{3T_s} \right] \quad (15)$$

The exergy efficiency is defined as the ratio of the receiver exergy rate to the rate of the concentrated solar radiation exergy and can be determined as follows:

$$\eta_{\text{ex.R}} = \frac{EX_R}{EX_D} = \frac{\dot{m} c_{\text{av}} \left[(T_{\text{out}} - T_{\text{in}}) - T_{\text{amb}} \ln\left(\frac{T_{\text{out}}}{T_{\text{in}}}\right) \right]}{n_d GA_{\text{ap}} \left[1 + \frac{1}{3} \left(\frac{T_{\text{amb}}}{T_s} \right)^4 - \frac{4T_{\text{amb}}}{3T_s} \right]} \quad (16)$$

The exergy factor is defined as the ratio of the receiver exergy rate to the receiver energy rate and can be represented by Eq. (17):

$$EX_f = \frac{EX_R}{E_R} = \frac{\dot{m} c_{\text{av}} \left[(T_{\text{out}} - T_{\text{in}}) - T_{\text{amb}} \ln\left(\frac{T_{\text{out}}}{T_{\text{in}}}\right) \right]}{\dot{m} c_{\text{av}} (T_{\text{out}} - T_{\text{in}})} \quad (17)$$

3. Uncertainty analysis

The uncertainties of the measurements in the experiment are dependent on the experimental conditions and the measurement instruments. An uncertainty analysis is performed on the receiver power E_R and the receiver exergy Ex_R , which are the most important derived quantities from the measurements when using the propagation of error method described by Moffat [31]. The uncertainty of the receiver power could be calculated by the following equation:

$$\delta E_R = \sqrt{\left(\frac{\delta E_R}{\delta \dot{m}}\right)^2 (\delta \dot{m})^2 + \left(\frac{\delta E_R}{\delta T_{out}}\right)^2 (\delta T_{out})^2 + \left(\frac{\delta E_R}{\delta T_{in}}\right)^2 (\delta T_{in})^2} \quad (17)$$

While the uncertainty of the receiver exergy rate is given by

$$\delta Ex_R = \sqrt{\left(\frac{\delta Ex_R}{\delta \dot{m}}\right)^2 (\delta \dot{m})^2 + \left(\frac{\delta Ex_R}{\delta T_{out}}\right)^2 (\delta T_{out})^2 + \left(\frac{\delta Ex_R}{\delta T_{in}}\right)^2 (\delta T_{in})^2 + \left(\frac{\delta Ex_R}{\delta T_{amb}}\right)^2 (\delta T_{amb})^2} \quad (18)$$

In the current study, the main uncertainty parameters are the mass flow rate (\dot{m}), the inlet temperature (T_{in}), and the outlet temperature (T_{out}). The relative uncertainty of the mass flow rate is given by the float flowmeter with the value of 2%. Therefore, $\delta \dot{m} = 2\% \times \dot{m} = \pm 0.001 \text{ kg/s}$. The uncertainty of the temperature is given by the K-type thermocouple with the value of $\delta T_{out} = \delta T_{in} = \pm 0.5 \text{ K}$.

The maximum experimental values for the receiver power and exergy rate are around 18.5 kW and 7.28 kW, respectively. The uncertainty of the receiver power is 0.372 kW, and the uncertainty of the receiver exergy rate is 0.147 kW. Overall, the overall uncertainty of the receiver power and exergy rate are 2.01% and 2.02%, respectively.

4. Results and discussion

Fig. 6 shows the variation of the solar irradiance (G) during a test period from 10:00 am to 13:30 pm. The experimental data were collected on November 6th, 2015, which falls in the local autumn season in Hangzhou, China. According to Fig. 6, it is shown that the solar irradiance fluctuates around 600 W/m^2 . The solar irradiance data increases slowly with time except two fast drops observed in the afternoon for about 15 mins. The reason could be due to the fact that two short periods of passing cloud occurred. From this figure, it can be seen clearly that the solar irradiance is almost stable and maintained at around 600 W/m^2 from 10:00 am to 12:00 pm. It is obviously that the stable solar irradiation condition is beneficial for analyzing the energy and exergy performance of the solar receiver. For this purpose, a test period of continuous 2 h from 10:00 am to 12:00 pm was selected. A dynamic acquisition system was used to record the parameters automatically during the test. The ambient temperature is maintained at around $25 \text{ }^\circ\text{C}$ during the experimental process. Fig. 7 shows the variation of the inlet pressure, outlet pressure and mass flow rate. As the design pressure of the solar receiver is 0.4 Mpa, the experiment should be conducted at the same pressure. Since the heating from the concentrated solar irradiation could lead to the rising of the internal pressure, the inlet valve is adjusted during the experimental process to ensure the solar receiver is working safety. Therefore, the mass flow rate fluctuates all the time. The average value of the mass flow rate is about 0.036 kg/s . In

the current study, the main purpose is to test the energy and exergy performance of the solar receiver under the fluctuating mass flow rate condition.

Fig. 8 presents the time series of air temperatures at the inlet and outlet of the receiver. The inlet temperature maintains nearly constant at about 42 °C. The outlet temperature rises very quickly initially, and achieves the highest temperature of 480 °C at the end of the experimental process. From 10:00 am to 10:30 am, it takes about half an hour to raise the solar receiver outlet temperature from 42 °C to 430 °C. After 10:30 am, the outlet temperature increases very slowly with the time. The first half an hour is used for preheating. It is due to the fact that the receiver tubes are surrounded by the insulation materials with high specific heat capability (C_p). It is noteworthy that the rising speed of the receiver efficiency is very high within the first 30 mins. This phenomenon is very important and should be stressed here since the sunshine is limited in the day time, and a quick start up can make the overall solar power generation system to generate more electricity. Therefore, the cost of the power generation will be lower and the investment recovery period could be shorter. There is also another interesting phenomenon in that the mass flow rate fluctuation has little effect on the solar receiver outlet temperature. It may be due to the reason that the porous metal is used as the heat absorbing core. The pore size is very small with the value about 0.34 mm. This small size pore could increase the heat transfer coefficient and area obviously. The heat transfer between the porous metal and the air is strong enough so that the air outlet temperature could be very close to the temperature of the

porous metal. Therefore, the effect of the mass flow rate fluctuation on the solar receiver outlet temperature is very small.

Fig. 9 presents a comparison of the power for the concentrated solar radiation and receiver power. For the case of the nearly constant solar irradiance of 600 W/m^2 , the concentrated solar radiation power (E_D) is maintained at around 22.5 kW with the fluctuation lower than $\pm 10\%$. In addition, the accurate control system can make sure the reflection focus is located at the aperture of the receiver. The red line shown in Fig. 9 is the receiver power during the testing period. For the first 10 mins, the solar receiver power (E_R) rise quickly from nearly 0 kW to 12 kW. After that, the value of E_R has the same trend as the mass flow rate with the time. In other words, the mass flow rate has a great influence on the solar receiver power. This can be easily explained by Eq. (3). As previously mentioned, the mass flow fluctuation has little influence on the value of c_{av} , T_{out} and T_{in} , so that the solar receiver power is mainly affected by the mass flow rate especially after the starting stage. The maximum solar receiver power is achieved at about 11:50am with the value of 18.5 kW.

Fig. 10(a) shows the time series of the solar receiver efficiency. It is found that when the solar receiver turns into steady state, the efficiency of the solar receiver can be above 55%. The peak value of the efficiency is 87%, and finally, the efficiency is maintained at around 60%. And it is also found that the value of $\eta_{th,R}$ has the same trend with the mass flow rate after the receiver entering into steady stage. In other

words, the energy efficiency is positively correlated with the mass flow rate as shown in Fig. 10(b). The main reason for this phenomenon can be explained by Eq. (10). As described above, the concentrated solar radiation power (E_D) is nearly maintained constant at around 22.5 kW, but the mass flow rate has great influence on the solar receiver power (E_R). Therefore, the ratio of E_R and E_D has a positive relationship with the mass flow rate. This is a very beneficial conclusion. Because in our experiment, the mass flow rate is obviously lower than the real solarized gas turbine system. So the efficiency of the real solarized gas turbine system will be very high. Correspondingly, the usage of the gas will be lower and the investment recovery period could be shorter.

Fig. 11 demonstrates the evolution of the heat loss factor (U'_L). At the starting point, U'_L is very high (1.17 kW/K) because of the receiver preheating, and then it drops very quickly within the first 5 mins. When the receiver works at steady state, the heat loss becomes lower and U'_L achieves the minimum value of 0.014 kW/K. In the current study, the heat loss mainly consist of the conduction heat loss, convection heat loss and radiative heat loss. Conduction heat loss could be reduced by using material with low thermal conductivity. In the present work, the receiver is surrounded by Aluminum silicate whose thermal conductivity is 0.06 W/(m · K). The Aluminum silicate can act as the thermal insulator to minimize the heat loss. The thermal convection between the solar receiver and ambient is very low as well, this is because the absorbing core is sealed in a pressurized cavity. As a result, only small

natural convection occurs around the external cavity of the receiver. It is noted that the use of the insulator could obviously reduce the natural convection. The radiative heat loss is also an important part of the heat loss, but it can be reduced by using small aperture, as shown in Fig 4. In the design of solar receiver, choosing an appropriate aperture diameter is very important for the receiver performance.

Fig. 12 shows the comparison between the receiver exergy (Ex_R) and the concentrated solar energy as well as the receiver energy. From this figure, the exergy rate and energy rate vary in a similar manner, the mass flow rate also has the same influence on the exergy rate. It is noted that the highest value of the exergy rate during the test period is around 7.28 kW, whereas the maximum energy rate can reach 18.5 kW. It can be concluded that the quality of the energy from the receiver is low due to a large amount of irreversible energy changes such as heat losses and the transfer of high quality solar energy to a fluid that is circulating at a relatively low temperature. From Eq. (13), it can be concluded that under the same temperature difference ($T_{out} - T_{in}$) and the same energy rate $\dot{m}c_{av}(T_{out} - T_{in})$ condition, increasing the receiver inlet temperature (T_{in}) can achieve higher exergy rate (Ex_R). This will be very helpful for the design of the solar power system. As a result, some recuperator or heat exchanger should be used in the inlet of the solar receiver to recover the waste heat and increase the solar inlet temperature.

Fig. 13 presents the comparison between the energy efficiency and exergy efficiency. It is shown from Fig. 13 that similar trends in the exergy efficiency and the

energy efficiency are obtained. The highest exergy efficiency is approximately 36%, whereas the highest energy efficiency is around 87%. This suggests that low quality energy obtained from the receiver. It is because the inlet temperature of the receiver is lower than 316 K, whereas the outlet temperature is very high and with the maximum value of 850 K. The temperature ratio (T_{out}/T_{in}) is very high so that too much exergy loss is observed. Fig.14 shows the exergy efficiency calculated by Eq. (16) varies with the inlet temperature. The calculating condition is $\dot{m} = 0.04\text{kg/s}$, $T_{out} - T_{in} = 400\text{K}$, $T_{amb} = 298\text{K}$. It is obvious that the exergy efficiency increases with the inlet temperature raises. Therefore, increasing the inlet temperature could be a potential way to increase the exergy efficiency.

Fig. 15 shows the exergy factor plotted as a function of the temperature difference between the outlet and inlet temperature of the receiver with a linear correlation fitted. The exergy factor is also usually used as a measure of the performance of the receiver. Obviously, as the temperature difference increases, the exergy factor also increases. With the temperature difference achieves 450 K, the exergy factor could be higher than 0.4. And this plot also suggests that a higher exergy factor can be obtained when high temperature difference is available. As seen from this figure, the highest exergy factor is 0.41 during the entire test.

5. Conclusions

This paper performed an experimental study to investigate the thermal performance of a pressurized volumetric solar receiver under real solar radiation

conditions. In order to design a high efficiency solar receiver, some important parameters such as different porous material, the size of the quartz window, the shape of the cavity, should be selected carefully. In the current work, a parabolic dish with solar tracker system is well designed and the obtained results are analysed using energy and exergy analyse method. Experimental results reveal that the solar irradiance is almost stable and maintained at around 600 W/m^2 from 10:00 am to 12:00 pm. It takes about half an hour to raise the solar receiver outlet temperature from 42°C to 430°C . After 10:30 am, the outlet temperature increases very slowly with the time. The mass flow rate fluctuation has little effect on the solar receiver outlet temperature. However, the mass flow rate has great influence on the solar receiver power, energy efficiency and exergy efficiency. The efficiency of the solar receiver can be above 55%. The peak value of the efficiency is 87%, and finally, the efficiency is maintained at around 60%. During the steady state, the heat loss becomes lower and U'_L achieves the minimum value of 0.014 kW/K . The highest exergy efficiency is approximately 36%, whereas the highest energy efficiency is around 87%. As the temperature difference increases, the impact of the exergy factor increases. The highest exergy factor is 0.41 during the entire test.

Acknowledgements

The authors would like to acknowledge the financial support from National Natural Science Foundation of China (No. 51206164).

References

- [1] Steinfeld A. 2005. Solar thermochemical production of hydrogen - a review. *Solar Energy*, 78:603-15.
- [2] Le Roux WG, Bello-Ochende T, Meyer JP. 2011. Operating conditions of an open and direct solar thermal Brayton cycle with optimised cavity receiver and recuperator. *Energy*, 36:6027-36.
- [3] Uri Fisher, Chemi Sugarmen, Arik Ring, Joseph Sinai, 2004. Gas Turbine “Solarization”-Modifications for Solar/Fuel Hybrid Operation, *J. Sol. Energy Eng.* 126(3), 872-878
- [4] Peter Heller, Markus Pfänder, Thorsten Denk, Felix Tellez, Antonio Valverde, Jesús Fernandez, Arik Ring, 2006. Test and evaluation of a solar powered gas turbine system, *Solar Energy*, 80(10), 1225-1230
- [5] Peter Schwarzbözl, Reiner Buck, Chemi Sugarmen, Arik Ring, Ma Jesús Marcos Crespo, Peter Altwegg, Juan Enrile, 2006. Solar gas turbine systems: Design, cost and perspectives, *Solar Energy*, 80(10), 1231-1240
- [6] Chen Lingen, Zhang Wanlin, Sun Fengrui, 2007. Power efficiency entropy-generation rate and ecological optimization for a class of generalized irreversible universal heat engine cycles. *Appl. Energy*, 84:512-25.
- [7] Matthew Neber, Hohyun Lee, 2012. Design of a high temperature cavity receiver for residential scale concentrated solar power. *Energy*, 47:481-487

- [8] Sehwa Lim, Yongheack Kang, Hyunjin Lee, Seungwon Shin. 2014. Design optimization of a tubular solar receiver with a porous medium, *Appl. Therm. Eng.* 62: 566-572.
- [9] Wei Wu, Lars Amsbeck, Reiner Buck, 2014, On the influence of rotation on thermal convection in a rotating cavity for solar receiver applications. *Appl. Therm. Eng.* 70: 694-704.
- [10] Buck R, Brauning T, Denk T, Pfander M, Schwarzbozl P, Tellez F. 2001. Solar-hybrid gas turbine-based power tower systems, *J. Sol. Energy Eng.* 124(1):2-9.
- [11] Hischier I, Hess D, Lipinski W, Modest M, Steinfield A., 2009. Heat transfer analysis of a novel pressurized air receiver for concentrated solar power via combined cycles. *J. Thermal Sci. Eng. Appl.* 1:1-6.
- [12] Hischier I, Hess D, Lipinski W, Modest M, Steinfield A, 2009. Heat transfer analysis of a novel pressurized air receiver for concentrated solar power via combined cycles. *ASME J. Therm. Sci. and Eng. Appl.*, Vol. 1 / 041002-1.
- [13] Nan Tu, Jinjia Wei, Jiabin Fang, 2014. Numerical study on thermal performance of a solar cavity receiver with different depths. *Appl. Therm. Eng.* 72: 20-28.
- [14] Wang M, Siddiqui K, 2010. The impact of geometrical parameters on the thermal performance of a solar receiver of dish-type concentrated solar energy system. *Renew. Energy*, 35:2501-13.

- [15] Shuang-Ying Wu, Lan Xiao, You-Rong Li, 2011, Effect of aperture position and size on natural convection heat loss of a solar heat-pipe receiver. *Appl. Therm. Eng.* 31 :2787-2796
- [16] Hachicha AA, Rodriguez I, Castro J, Oliva A. 2013, Numerical simulation of wind flow around a parabolic trough solar collector. *Appl. Energy.* 107:426-37.
- [17] Hachicha AA, Rodriguez I, Capdevila R, Oliva A, 2013, Heat transfer analysis and numerical simulation of a parabolic trough solar collector. *Appl. Energy.* 111:581-92.
- [18] Storch HV, Roeb M, Stadler H, Stadler H, Sattler C, Hoffschmidt B, 2016, Available online Efficiency potential of indirectly heated solar reforming with different types of solar air receivers. *Appl. Therm. Eng.* 92:202-209.
- [19] Flesch R, Stadler H, Uhlig R, 2014. Numerical analysis of the influence of inclination angle and wind on the heat losses of cavity receivers for solar thermal power towers, *Solar Energy*, 110:427-37.
- [20] Yu Z, Feng Y, Zhou W, Jin Y, Li M, Li Z, Tao W., 2013, Study on flow and heat transfer characteristics of composite porous material and its performance analysis by FSP and EDEP. *Appl. Energy*, 112:1367-75.
- [21] Tu N, Wei J, Fang J, 2015. Numerical investigation on uniformity of heat flux for semi-gray surfaces inside a solar cavity receiver, *Solar Energy*, 112:128-43.

- [22] Capeillere J, Toutant A, Olalde G, Boubault A, 2014. Thermomechanical behavior of a plate ceramic solar receiver irradiated by concentrated sunlight, *Solar Energy*, 110: 174-87.
- [23] Wang F, Tan J, Ma L, Shuai Y, Tan H, Leng Y, 2014. Thermal performance analysis of porous medium solar receiver with quartz window to minimize heat flux gradient, *Solar Energy*, 108: 348-59.
- [24] Roldan MI, Valenzuela L, Zarza E. 2013, Thermal analysis of solar receiver pipes with superheated steam. *Appl. Energy*, 103:73-84.
- [25] Jianqin Zhu, Kai Wang, Hongwei Wu, Dunjin Wang, Juan Du, A.G.Olabi, 2015, Experimental investigation on the energy and exergy performance of a coiled tube solar receiver, *Applied Energy*, 156: 519-527
- [26] Kai Wang, Hongwei Wu, Dunjin Wang, Yongsheng Wang, Zhiting Tong, Feng Lin, AG Olabi, 2015, Experimental Study on a Coiled Tube Solar Receiver under Variable Solar Radiation Condition, *Solar Energy*, 122: 1080–1090
- [27] Mawire A, Taole S, 2014. Experimental energy and exergy performance of a solar receiver for a domestic parabolic dish concentrator for teaching purposes. *Energy Sustain. Dev.* 19:162-9.
- [28] Macphee D, Dincer I, 2009. Thermal modeling of a packed bed thermal energy storage system during charging. *Appl. Therm. Eng.* 29:695-705.

- [29] Padilla RV, Fontalvo A, Demirkaya G, Martinez A, Quiroga AG, 2014, Exergy analysis of parabolic trough solar receiver. *Appl. Therm. Eng.* 67:579-586.
- [30] Petela R, 2003. Exergy of undiluted thermal radiation. *Solar Energy*, 74:469-88.
- [31] Moffat RJ, 1988, Describing the uncertainties in the experimental results. *Exp. Therm. Fluid Sci.*, 1:3-17

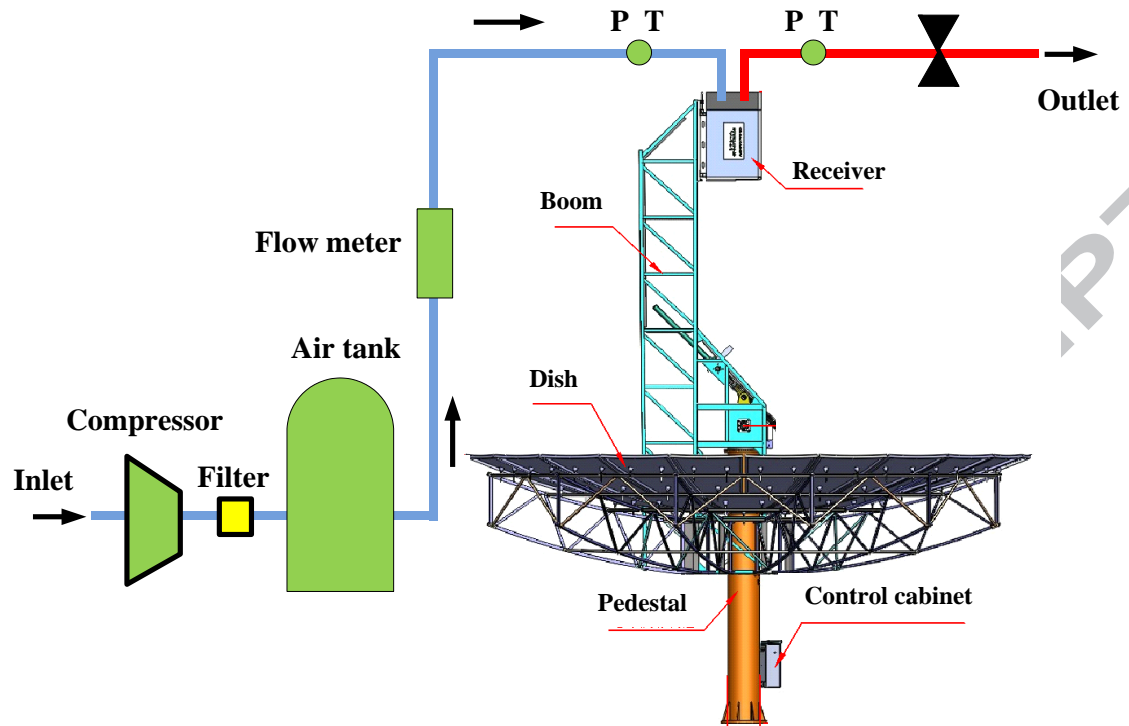


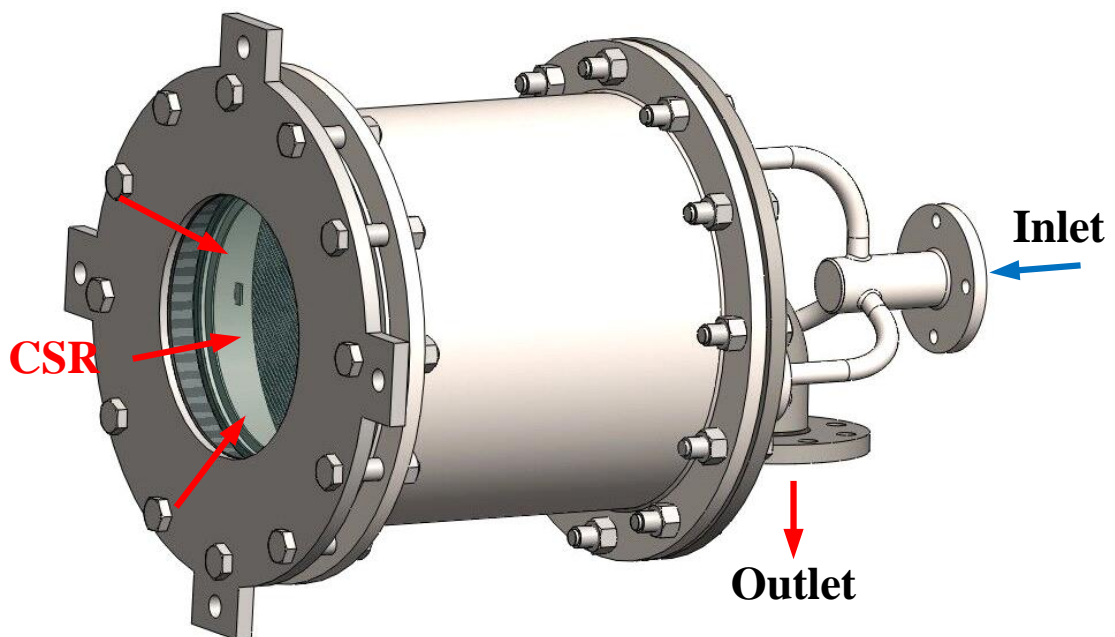
Fig. 1. Schematic drawing of experimental test rig.



Fig. 2. Parabolic dish.



Fig. 3. Protecting shield under the concentrated solar radiation.



(a)

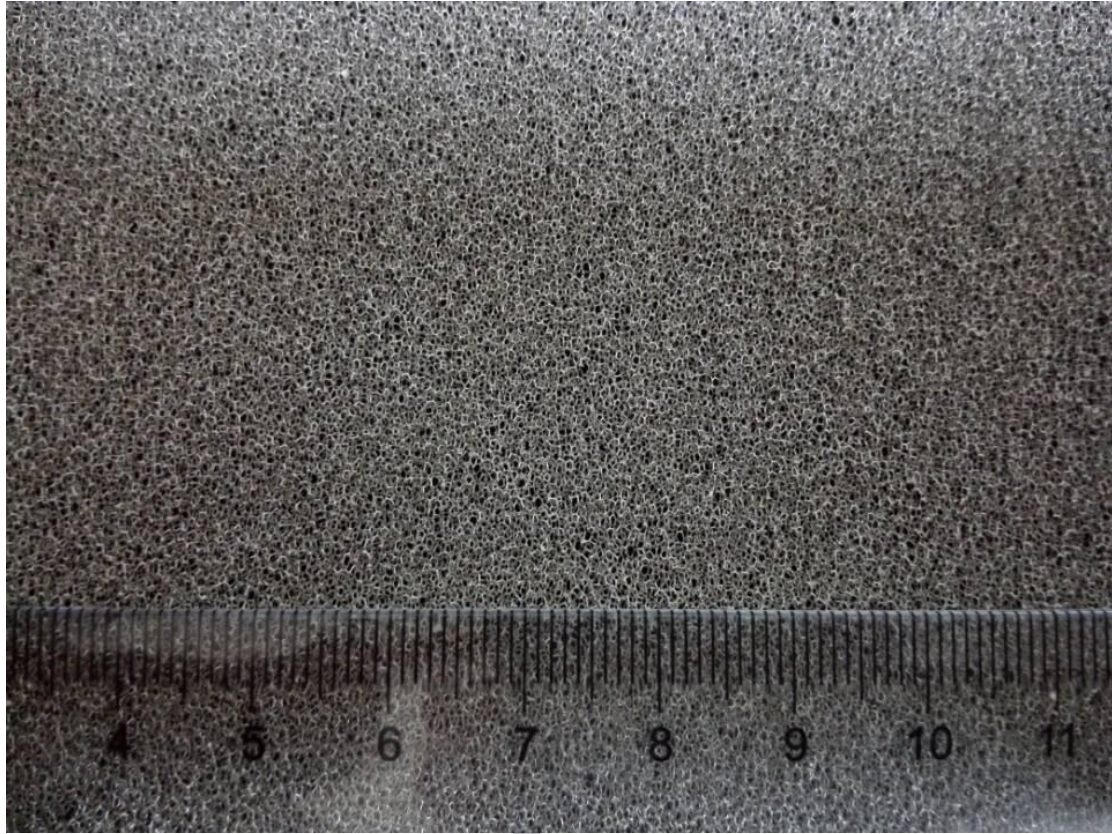


Fig.5. Nickel foam.

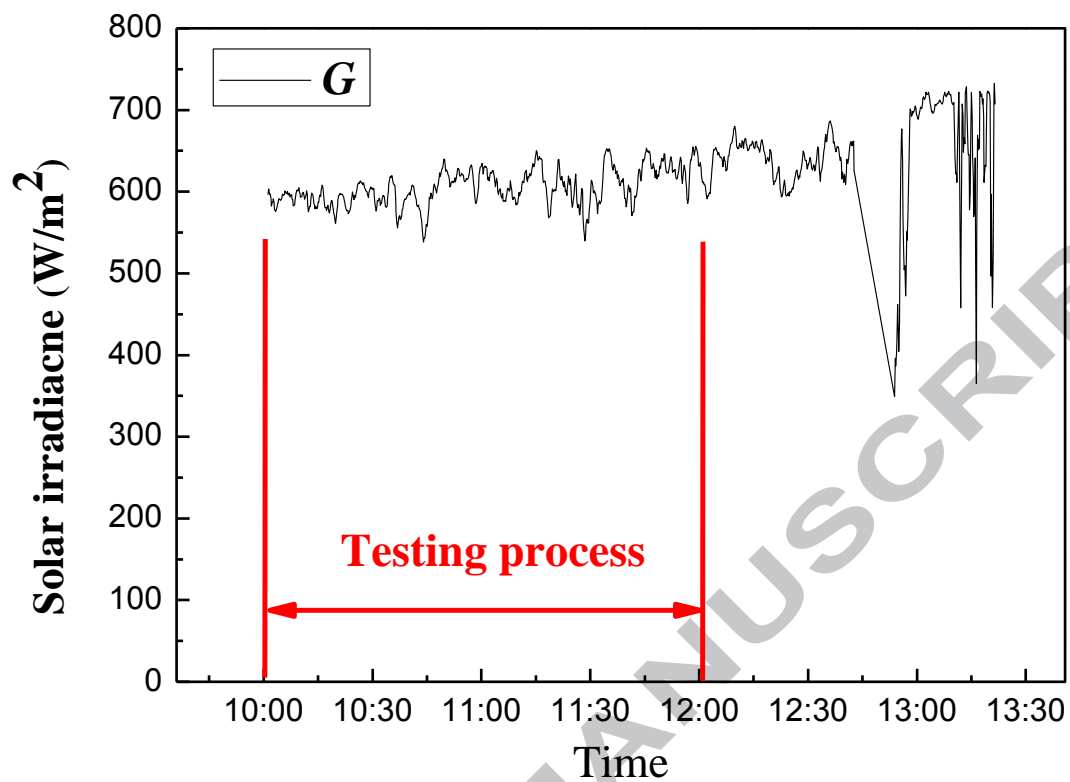


Fig. 6. Solar irradiance data during the day.

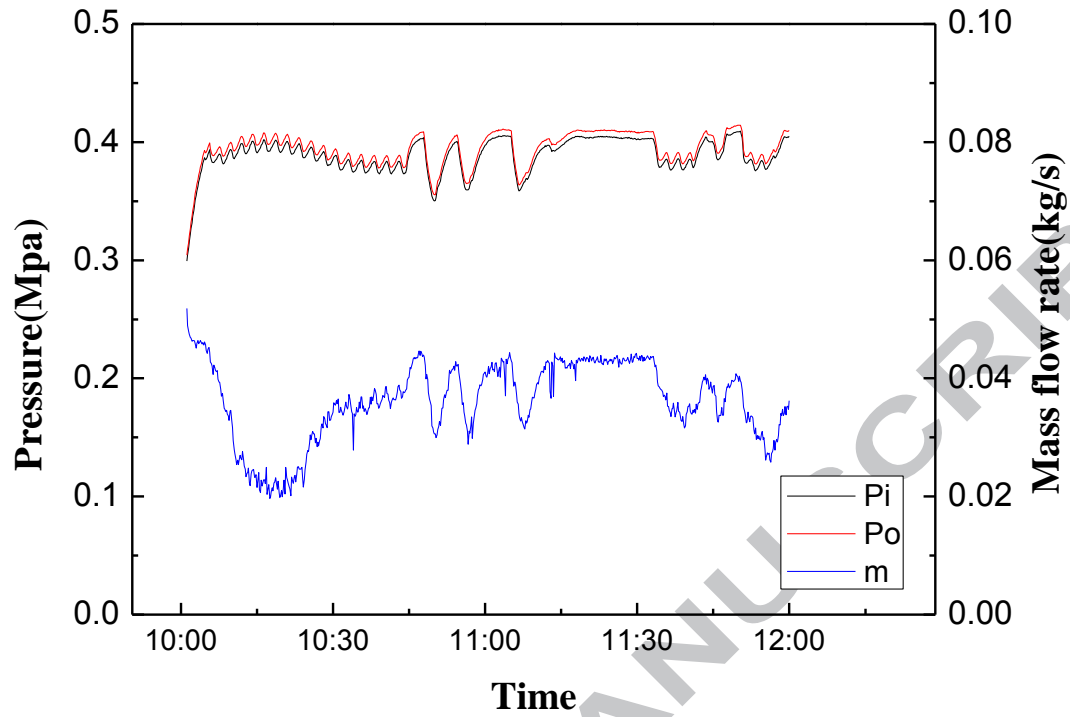


Fig. 7. Variation of the inlet pressure, outlet pressure and mass flow rate.

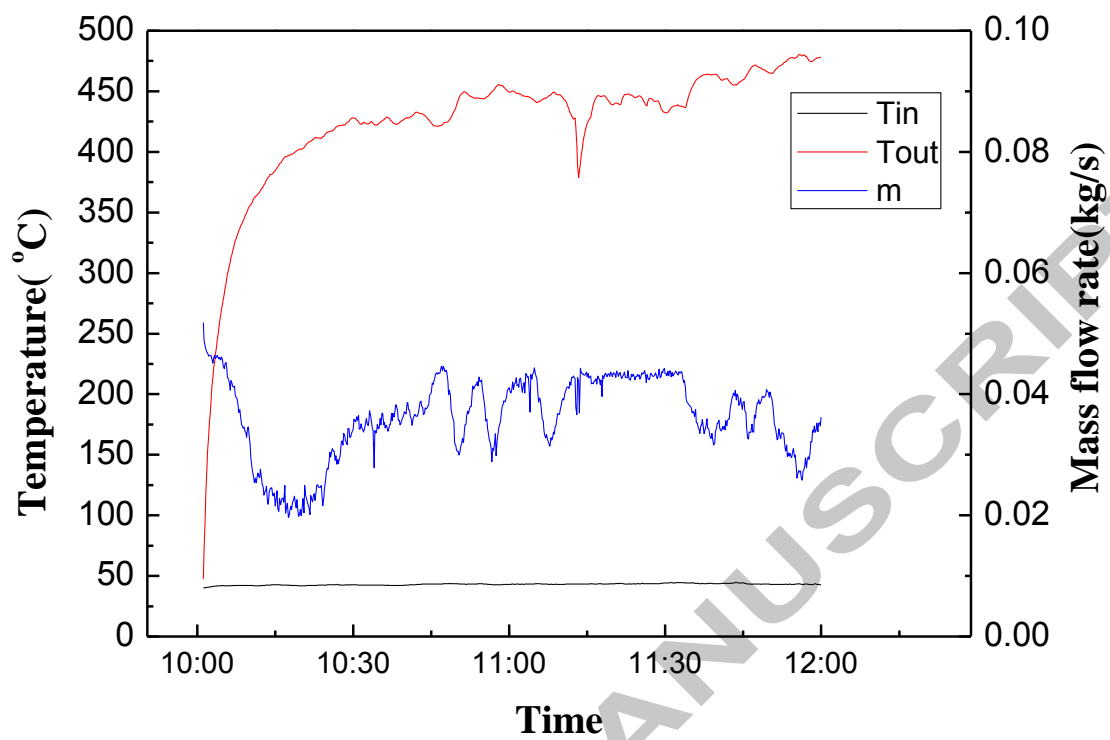


Fig. 8. Variation of the inlet temperature, outlet temperature and mass flow rate.

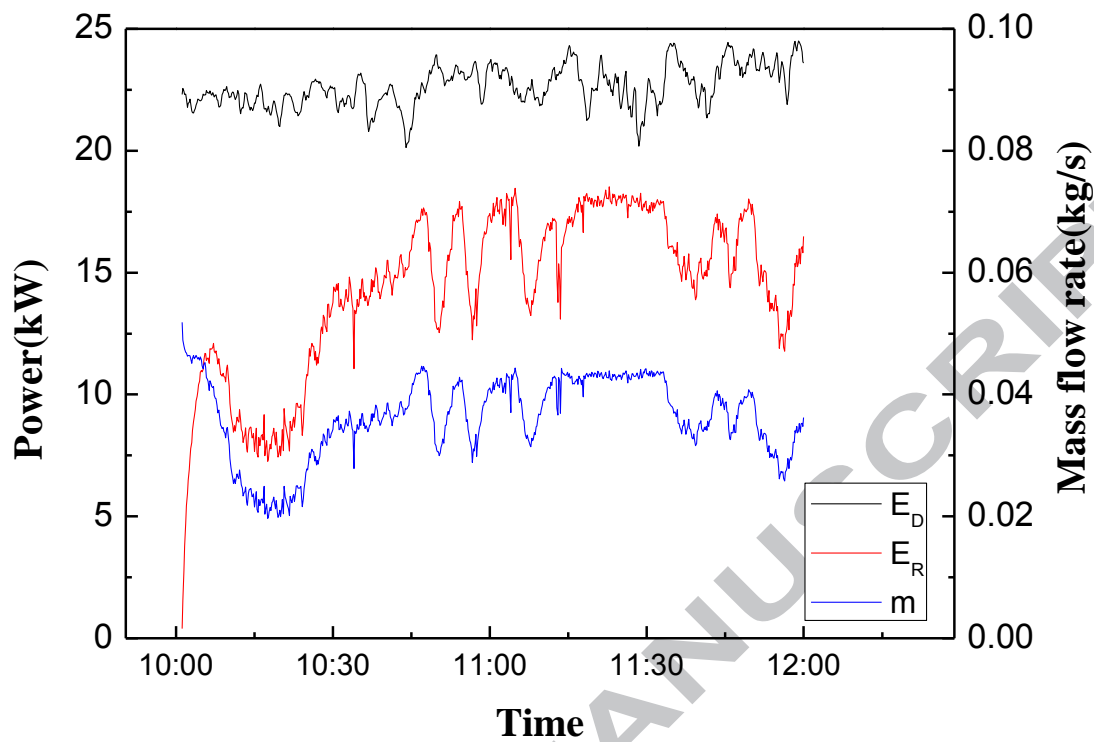


Fig. 9. Variation of the dish power, receiver power and mass flow rate.

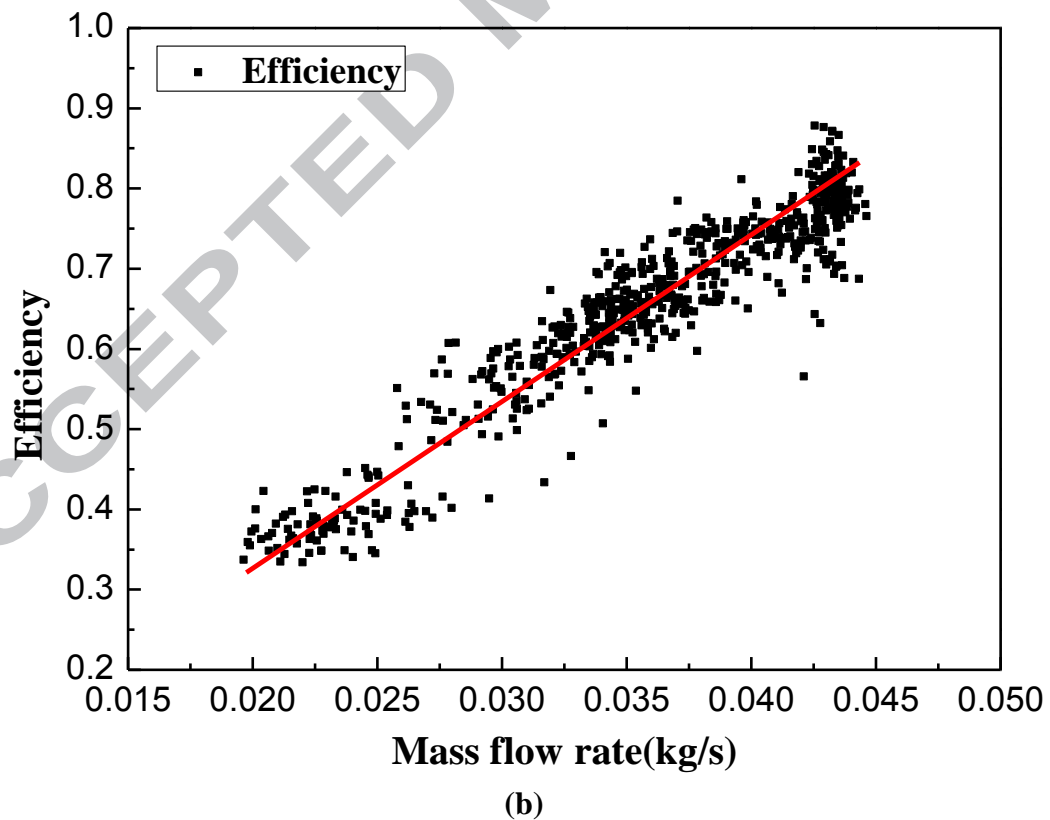
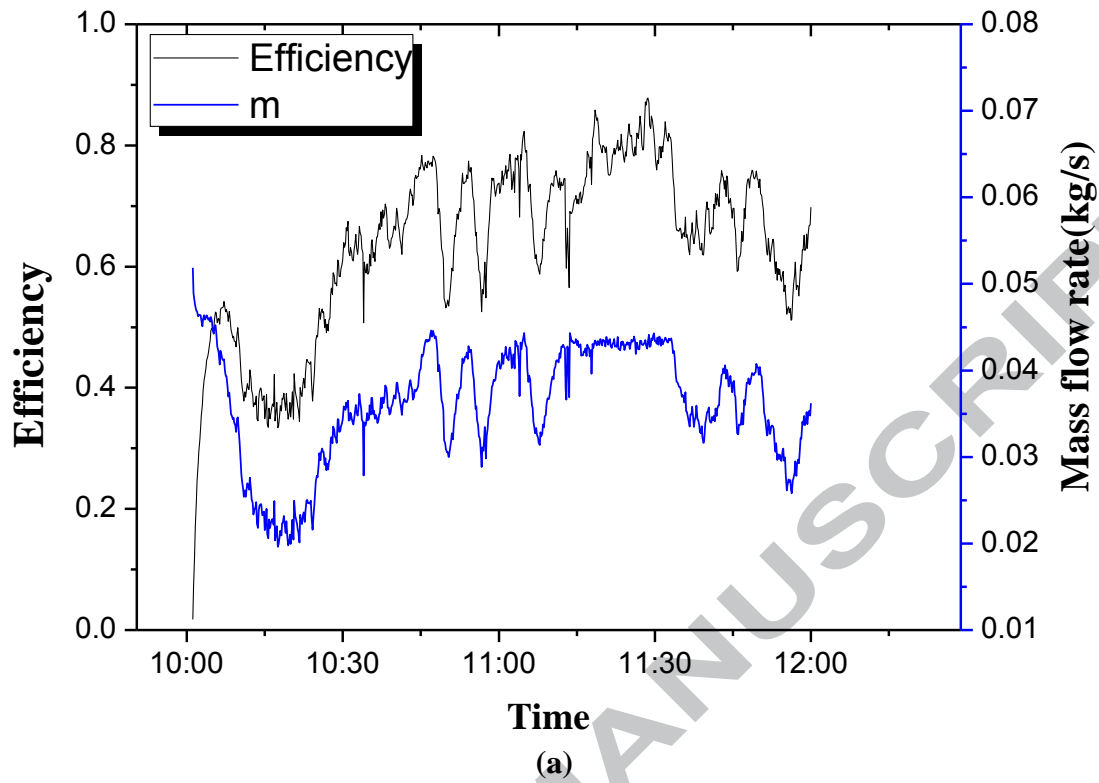


Fig. 10. Efficiency results. (a) during the test period, (b) efficiency vs. mass flow rate.

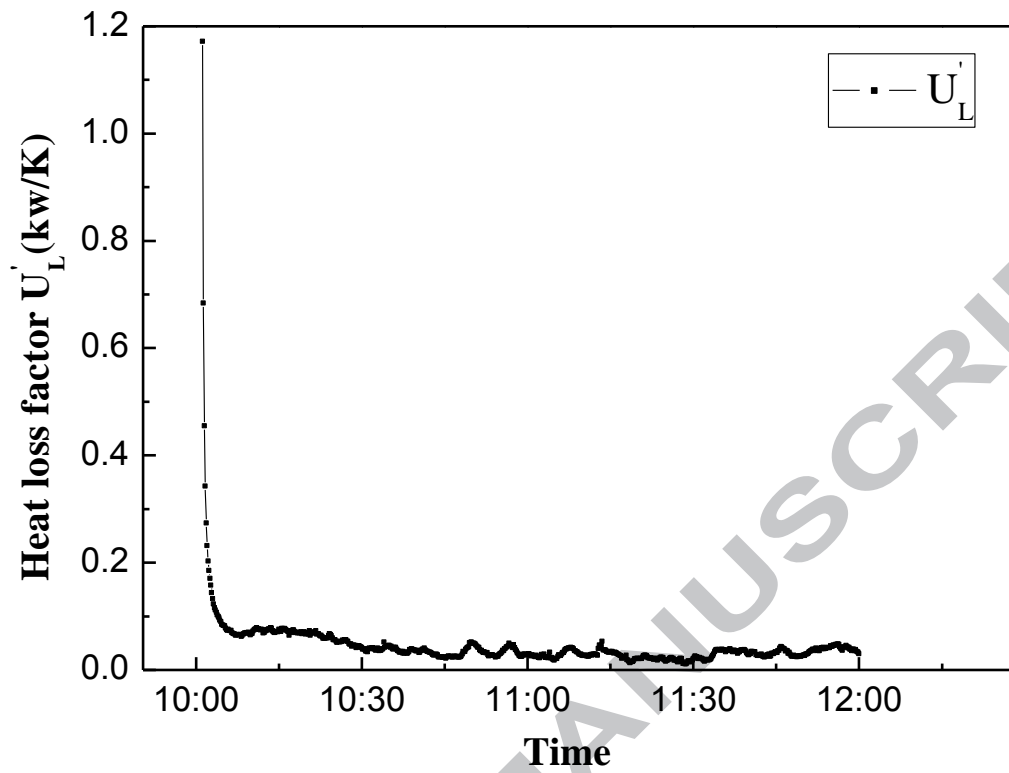


Fig. 11. Heat loss factor profile during the test period.

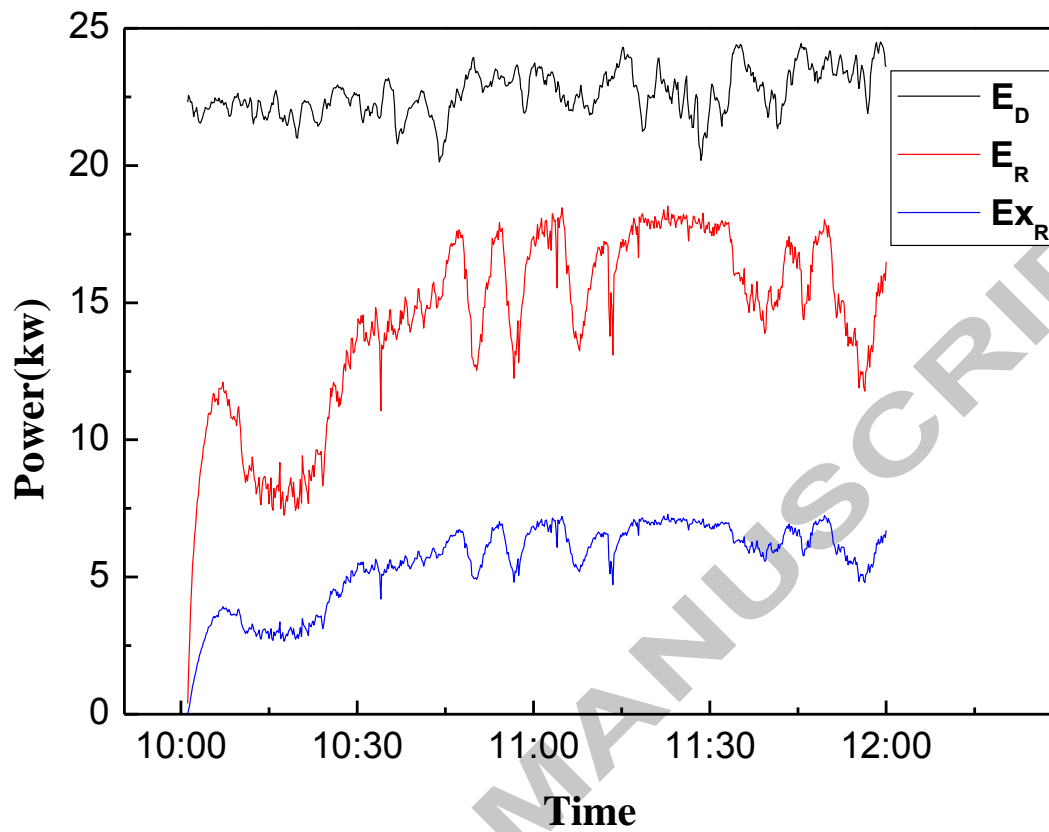


Fig. 12. Variation of the power for the receiver energy and exergy during the test period.

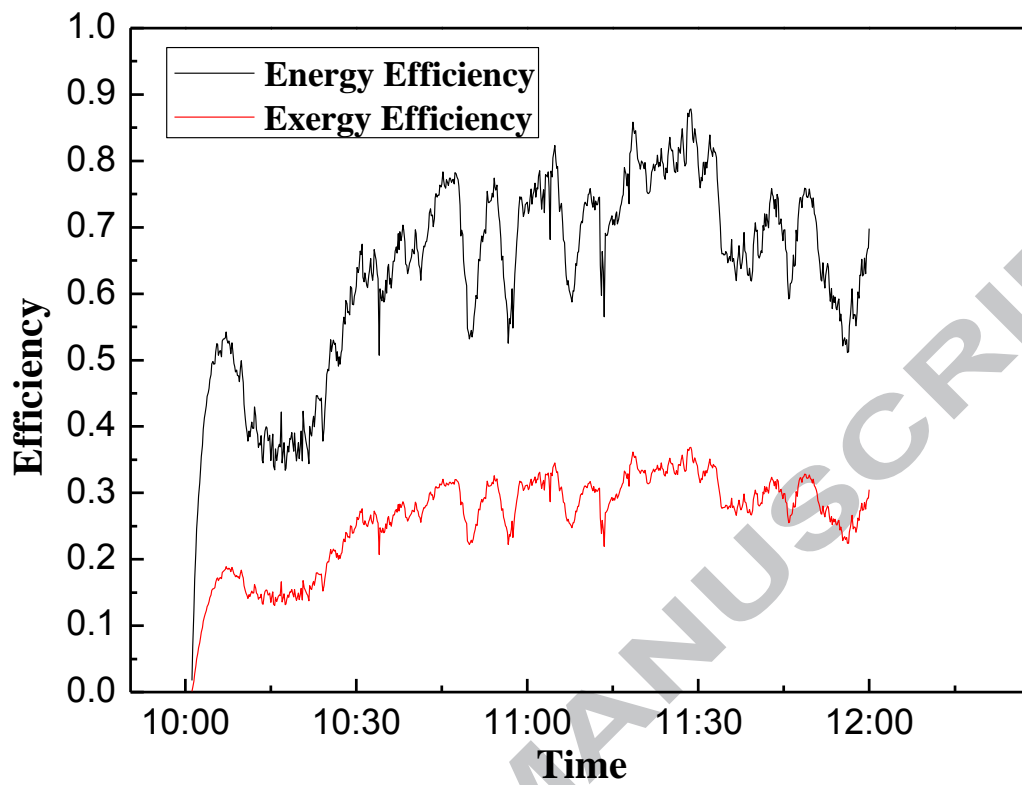


Fig. 13. Energy and Exergy efficiency profile during the test period.

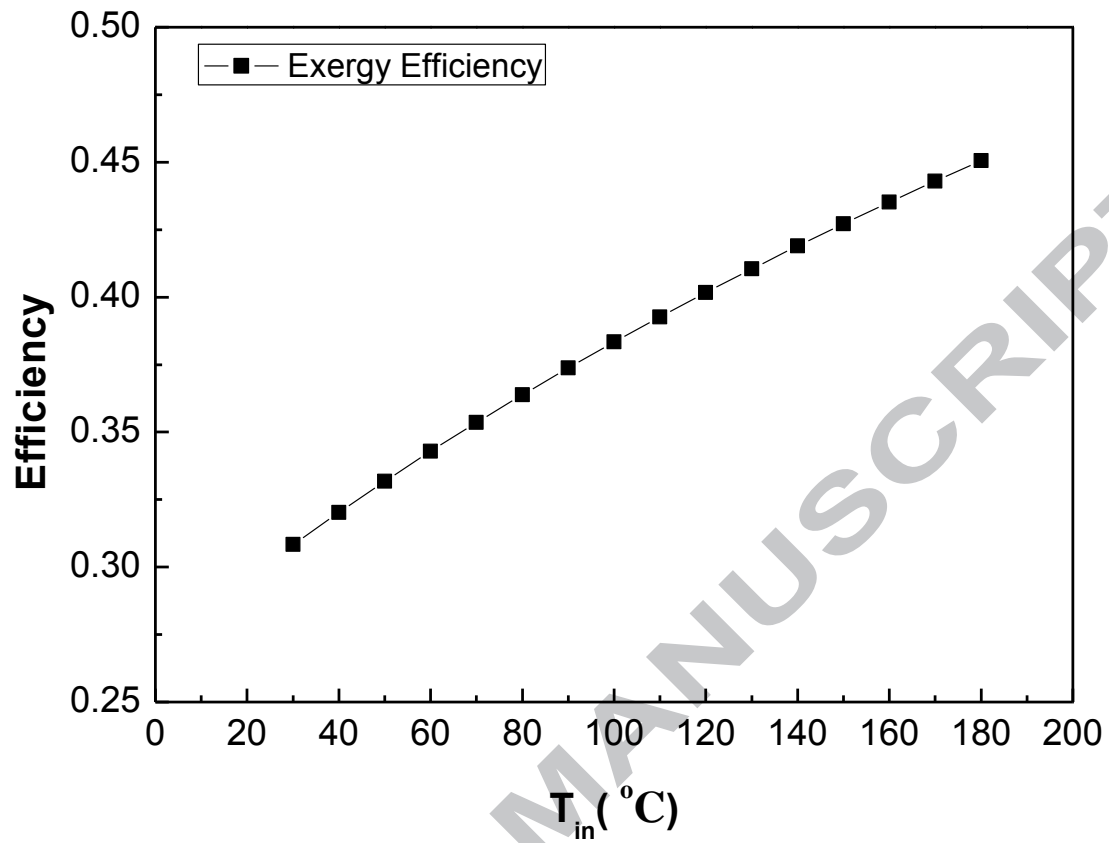


Fig. 14. The exergy efficiency variation with inlet temperature.

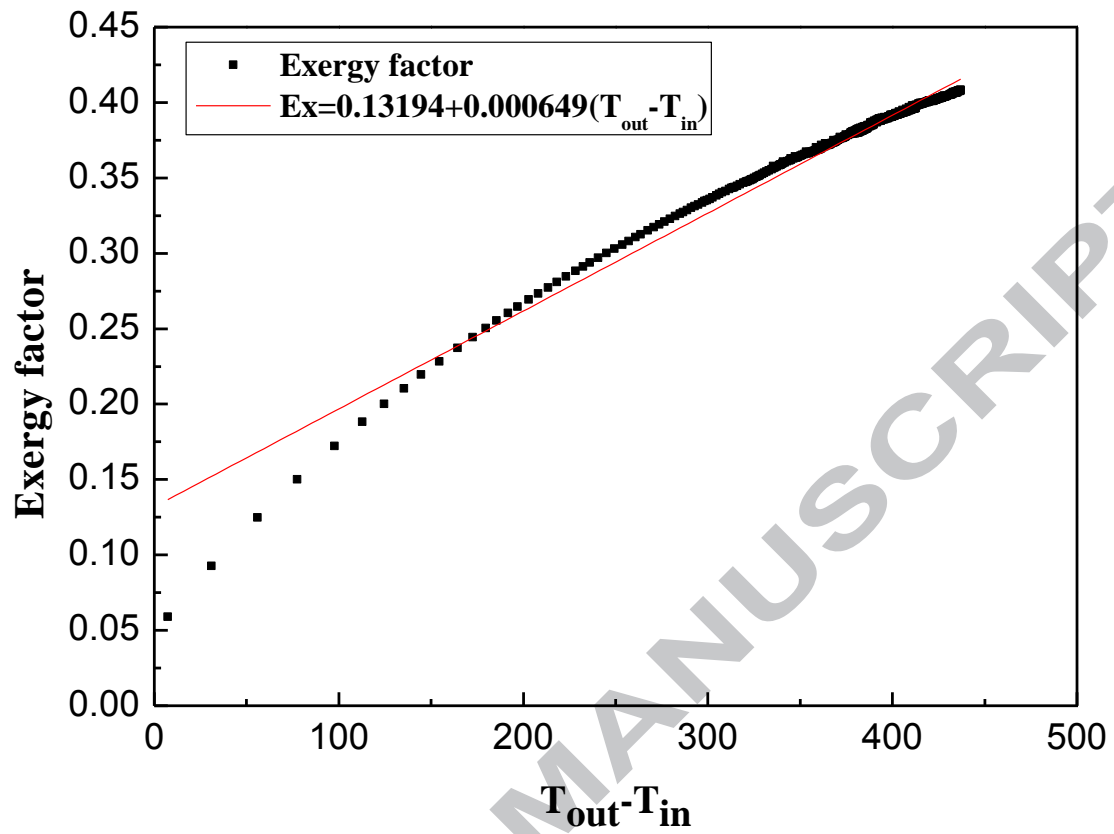


Fig. 15. The effect of temperature difference on the exergy factor.

Table 1

Dish design parameters.

Parameters	Value (unit)
Effective aperture area of dish (A_{ap})	44 m ²
Project area (A_p)	90 m ²
Focus length(L_d)	6.7m
Rim angle(α)	45°
Focus point diameter (D_f)	0.18 m
Concentration ratio (r_c)	1750
Parabolic dish combined optical efficiency (η_d)	85%
Mirror number	40
Slop error	0.5 mrad